






# Evaluation of Wind Power Potential in Lom and Djerem: The Case of the City of Bertoua in East Cameroon Region

Doka Baza Gilbert<sup>1,2</sup>, Jean Benjamin Bidias<sup>1</sup> , Arnel Duvalier Pene<sup>2</sup>, Soumeiya Halimatou<sup>2</sup>,  
Bang Titti Paul Roland<sup>2</sup>, Kitmo<sup>1</sup> , Dieudonné Kidmo Kaoga<sup>1</sup>, Nsouandélé Jean Luc<sup>1,3</sup>

**Abstract:** The main sources of energy production in Cameroon remain hydropower and thermal power plants using fuel and gas. However, in recent years, it has been experiencing an imbalance that creates a mismatch between production and consumption. It is therefore of great importance to explore new sources of energy such as wind energy. In an effort to seek other sources of energy, we conducted this study aimed at assessing the wind potential in the Lom and Djèrem Department in the city of Bertoua. To achieve this, data obtained from the Bertoua airport were processed using the Weibull distribution, the wind distribution density and express the statistical estimation of wind energy potential at different altitudes of the site (annual energy density average of 60.97 kWh/m<sup>2</sup>/year), which will facilitate the installation of a wind farm in this locality. Given the existing wind energy potential, its use for the development of electric energy in the region seems somewhat suitable. An advantageous solution for Cameroon in general and the East region is the recovery and transformation of wind energy into electric energy, with a YDF-1500-87 CNYD type wind turbine guaranteeing a production of 82.66 kW at 100 m altitude in the month of January. Next, we determined the wind direction to position the wind turbines at the site. Finally, an assessment of the prediction of the electrical energy produced is made while relying on the careful selection of wind turbines and their load factors.

**Keywords:** Evaluation, Wind potential, Electrical energy, Weibull distribution, Wind turbines.

## History

Received: 20-12-2025;

Revised: 03-06-2026;

Accepted: 03-06-2026



Doka Baza Gilbert

[dokabazagilbert@gmail.com](mailto:dokabazagilbert@gmail.com)

<sup>1</sup>Department of Renewable Energy, National Advanced School of Engineering of Maroua, University of Maroua, PO Box 58 Maroua, Cameroon.

<sup>2</sup>Department of Renewable Energy, University Institute of Technology, University of Ngaoundéré, PO Box: 455 Ngaoundéré, Cameroon.

<sup>3</sup>Department of Energy, National Advanced School of Engineering of Douala, University of Douala, Douala, Cameroon.

## 1. Introduction

The need for electrical energy has become a global problem because of the depletion of natural resources such as coal, oil, bauxite, and many others. This has led many countries around the world to turn to renewable energies. But even though the potential for renewable energy is abundant in some places around the world, the problem of harnessing it remains. In Cameroon, for example, after the use of thermal power plants, it was realized that they were costing the Cameroonian government too much money and were also a source of air pollution. The production of thermal energy emits greenhouse gases such as CO<sub>2</sub> and sulfur that promote global warming and the destruction of the ozone layer [1 - 2]. The work of kidmo et al, [3], carried out in 2014, shows that it is possible to implement a high capacity power plant in Far North Cameroon. Work has also

been carried out in other countries on the same energy issues. It deals with the optimization of a wind power plant, while the optimization work focuses on a photovoltaic plant. Nowadays, most of Cameroon's leaders are seeking not only to make electrical energy accessible to everyone but also to satisfy the demand for electrical energy [4], which is becoming abundant, even to keep certain industrial companies running. Some studies have investigated the feasibility and profitability of wind power systems, while others are looking at photovoltaic systems and biomass systems. But in Cameroon, photovoltaic energy is more easily exploitable than wind power: in some regions of Cameroon, the wind is not strong enough to turn the turbines. And yet, these localities should benefit just as much as those where the wind is strong. The East region is one such area, with low wind speeds [4]. And to study the feasibility of setting up a wind power plant in this locality and to study the feasibility of setting up a wind power plant in the locality of East Cameroon. The work in this article focuses on the evaluation of the deposit before seeing how to determine the capacity of a wind power plant able to meet either the growing demand in the locality of Bertoua or partially the needs of certain households in the Eastern region. This work begins with a review of the literature on wind power in general and presents the energy and wind potential in Bertoua. After exploiting the climatic data for this region of Cameroon, an assessment of the energy capacity is determined by evaluating the wind speed from 1.55 m to 2.55 m for an altitude of 10 m. In addition, wind power is extrapolated to a height of 100 m. It's also worth pointing out that the NASA website already provides climatic parameters from 10 m upwards, including sunshine, wind speed, relative humidity, air mass density and ground roughness for each location.

In 2020, Cameroon's electricity production park recorded an installed capacity of 1529 MW distributed amongst hydroelectricity (61.7%) MW), thermal (24.1%), gas (14.1%) and solar panel (0.1%) power generation plants. Thermal power plants using heavy and light fuel oil represent the second largest source of energy production in Cameroon, both in the interconnected and isolated networks. They allow not only to compensate for energy deficits not covered by the active hydroelectric plants, but also to improve the voltage profiles. The problem of the energy deficit

arises when only 63.5% of the Cameroonian population has access to electricity. Demand is estimated at 1379 MW in 2021, for an offer of 1047 MW. That is a deficit of around 330 MW. Growth in demand is estimated at 7.5%/year. Today, there are new renewable energy solutions to the problem of load shedding and global warming, such as the use of renewable resources like connecting a photovoltaic plant and/or wind farm to the grid. With a view to finding solutions to these problems, we assessed the wind energy potential in the Lom et Djérem region, and more specifically in the town of Bertoua [4]. Among renewable energy resources, wind power has long been used worldwide. It's inexhaustible, non-polluting and free. The basic principle of this technology is to transform the wind's energy into sufficient mechanical power to pump water or generate electricity [5]. The exact determination of the wind energy potential, the modeling and simulation of the production of electrical energy adapted to the needs, both quantitative and qualitative, of any installation from the wind, will be the subject of work.

Specifically, we had to:

- Take hourly wind data readings at the site.
- Define the velocity distribution density function at the site.
- Model and simulate the production of electrical energy.
- Estimate the wind power available and recoverable in a stable manner over the course of a day and over the course of a year, as a function of altitude;

Consequently, this study aims to evaluate both the credibility and the variability of energy model simulations for wind turbines in Bertoua, using the Weibull distribution model as a reference to assess the performance of the models as well as to project production according to heights to improve energy planning and make relevant and informed policy decisions. For this study, the processed data were provided by Bertoua International Airport. After presenting the introduction, Section 2 presents the different methods that allowed us to obtain the results of this article, Section 3 presents the results and conclusions in Section 4.

## 2. Methods

Bertoua is a town in Cameroon's Lom-et-Djérem department, in the East region, which became the Bertoua Urban Community in 2008. The city is 350 km from Yaoundé. Bertoua is the regional capital of the East, Cameroon's largest forest region. Geographic coordinates of the locality will be taken from a GPRS, are,

- Latitude: 4°34'38" NORTH
- Longitude: 13°41'04" EAST
- Altitude: 665m

Fig. 1 below shows us the aerial view of the study site.



Fig. 1: Bertoua map

### 2.1. Bertoua's wind energy potential

Wind speed is the key factor in sizing and assessing the power output of wind turbines on a site. Today, there are countless systems for measuring and recording wind speed and direction on site, over periods ranging from one to ten years. Our monthly wind speeds for the eastern region were obtained by direct measurement at the Bertoua airport site. For this work, we contacted the Bertoua airport, which provided us with wind speed data. These daily speeds were measured using an anemometer installed at a height of ten meters above ground level at Bertoua airport. To carry out a possible study in the eastern region of Cameroon. These velocity data will be very important for modeling electricity generation parameters in this region.

### 2.2 Wind speed average and standard deviation

After obtaining the real values, we used Equation (1) and equation (2) [2] [6] to determine the average monthly wind speed  $v_m$  and the standard deviation  $\sigma$ .

$$v_m = \frac{1}{N} (\sum_{i=1}^N v_i) \quad (1)$$

$$\sigma = \left[ \frac{1}{N-1} \sum_{i=1}^N (v_i - v_m)^2 \right]^{1/2} \quad (2)$$

Where,

$v_m$ : wind speed average (m/s)

$N$ : number of measured hourly wind speed data.

$\sigma$  = standard deviation of the observed data (m/s)

$v_i$  = hourly wind speed (m/s)

### 2.3 Weibull Distribution

Since it's difficult to manipulate all the data relating to a wind frequency distribution, it's more suitable for theoretical considerations to model the histogram of wind speed frequencies by a continuous mathematical function than by a discrete table of values. We can therefore opt for the Weibull model. For periods ranging from a few weeks to several years, the Weibull function is a reasonable representation of observed speeds [5], [7]. To calculate the performance of a wind generator operating on a given site, we first need to equate the variation in energy potential characterized by its speed [7]-[11]. Among the mathematical models used in wind energy, the statistical model of the Weibull distribution is the most appropriate for describing the variation in wind speed. This model is mainly defined by the distribution function, which can be written as equation (3) [9], [11]-[13].

$$F(V) = 1 - \exp \left[ - \left( \frac{V}{c} \right)^k \right] \quad (3)$$

The Weibull distribution is expressed mathematically by its probability density function  $f(V)$  given by equation (4) [14 - 15],

$$f(V) = \left( \frac{k}{c} \right) \left( \frac{V}{c} \right)^{k-1} - \exp \left[ - \left( \frac{V}{c} \right)^k \right] \quad (4)$$

Where,

$f(V)$  represents the frequency of occurrence of wind speeds.

### 2.4 Calculation of Weibull parameters

The Weibull parameters  $c$  and  $k$  provide direct access to the characteristics of the wind potential. They can be calculated using the following two empirical expressions, equation (5) and (6) [16 - 21].

$$k = \frac{\sigma^{-1.089}}{v} \quad (5)$$

$$C = \frac{v}{\tau(1+\frac{1}{k})} \quad (6)$$

Where:

$\sigma$  = standard deviation of the observed data.

$\tau$  = Gamma function

## 2.5 Speed Extrapolation

In order to obtain adequate wind speeds for the operation of wind turbines, extrapolations are made to increase the wind speed as in the equation (7-9), [22] [7].

$$V(Z_2) = V(Z_1) \left(\frac{Z_2}{Z_1}\right)^\alpha \quad (7)$$

$$\alpha = \frac{1}{\ln\left(\frac{Z}{Z_1}\right)} - \left(\frac{0.0881}{1-0.00881 \ln\left(\frac{Z}{Z_1}\right)}\right) \ln\left(\frac{V(Z)}{6}\right) \quad (8)$$

$$\bar{Z} = \sqrt{Z_1 Z_2} \quad (9)$$

Where,

$V(Z_2)$ : wind speed at the height to be extrapolated  $Z_2$

$V(Z_1)$ : wind speed available at  $Z_1$  height angle

$Z_2$ : the desired height angle

$Z_1$ : 10 m height angle

$\alpha$ : power law exponent

The exponent of the power law is equal to 1/7

We extrapolated to heights of 100 m to better capture the wind's energy. After assessing the potential of the locality, we sized our wind generator according to its various parts.

## 2.6 Extrapolation of Weibull parameters as a function of height

With the  $K$  and  $C$  parameters calculated at 10 meters above ground level, we can extrapolate them according to the height of the site where we want to install the wind turbines. To do this, we use the following equation (10), equation (11) and equation (12) [3], [13]:

$$n = (0.37 - 0.088 \ln(C_{10})) \quad (10)$$

$$k_z = \frac{k_{10}}{1-0.00881 \ln\left(\frac{Z}{10}\right)} \quad (11)$$

$$C_z = C_{10} \left(\frac{Z}{Z_{10}}\right)_n \quad (12)$$

Where,

$z$ , represents the height at which the wind turbines are to be installed.  $C_z$  and  $K_z$ , the corresponding parameters.

## 2.7 Wind power and the Betz limit

### 2.7.1 Wind power densities

This is used to estimate the recoverable power at a site. It is obtained by equation (13) [23].

$$WPD = p(v) = \frac{P(V)}{S} T = \frac{1}{2} \rho V^3 \Gamma(x) \quad (13)$$

$\Gamma$ , is a function that characterizes the shape of the frequency distribution and the asymmetry of the speed frequency distribution. It is given by equation (14).

$$\Gamma(x) = \int_0^\infty t^{x-1} \exp(-t) dt = (\sqrt{2\pi x})(x^{x-1})(e^{-x}) \left(1 + \frac{1}{12}x + \frac{1}{288}x^2 + \frac{139}{51840}x^3 + \dots\right) \quad (14)$$

Wind Energy Density (WED) is a very important parameter, quantifying the energy produced over a time  $T$  by the wind turbines or wind farm. Note that the time  $T$  depends on the availability factor and the load factor. Its formula equation (15), is as follows [24 - 25].

$$WED = p(v)T = \frac{P(V)}{S} T = \frac{1}{2} \rho V^3 \Gamma(x) T \quad (15)$$

### 2.7.2 Power

An air density  $\rho$ [kg/m<sup>3</sup>], moving at a velocity  $v$ [m/s], contains a power per unit area perpendicular to the direction of flow (specific power): Its formula equation (16) is as follows,

$$P_0 = \frac{1}{2} \cdot \rho \cdot V^3 \quad (16)$$

$P_0$  at W/m<sup>2</sup>

For an area  $S$  (m<sup>2</sup>) swept by the effective aerodynamic length of the blades, the power  $P_0$  is (17),

$$P_0 = \frac{1}{2} \cdot \rho \cdot S \cdot V^3 \quad (17)$$

$P_0$  at (W) is given by (18),

$$\text{Where } S = \frac{\pi \cdot D^2}{4} \quad (18)$$

$D$  is the helix diameter and  $\pi$  is a constant equal to 3.14.

### 2.7.3 Theoretical recoverable power: the Betz limit

According to Betz, under ideal rotor and wind conditions:

- The rotor has no mechanical or aerodynamic losses.
- Air is incompressible and frictionless.
- The flow before and after is laminar.

The maximum wind power  $P_{wmax}$  transferred to the rotor is calculated as follows in (19),

$$P_{wmax} = \frac{16}{27} \cdot P_0 = 0.5926 \cdot P_0 \quad (19)$$

Where  $\frac{16}{27} = C_p$  the theoretical power coefficient or Betz limit

Under normal conditions (temperature 10°C, pressure 1 bar), the air density  $\rho$  is of approx. 1.25 kg/m<sup>3</sup>, as (20).

$$P_{wmax} = 0.29 \cdot D^2 \cdot V^3 \quad (20)$$

### 2.8 Load Factor

Turbine selection is a complex business. If you don't choose the right turbines, they won't be able to produce the energy you need. We avoid this difficulty by calculating the load factor before selecting a turbine. To calculate the load factor, we use the relationship in equation (18). This formula takes 05 parameters into account. Two are site-dependent (shape factor  $K$  and scale factor  $C$ ) and three are supplied by the turbine manufacturer (starting speed  $V_s$ , nominal speed  $V_N$  and stopping speed  $V_A$  of the turbine) [23], [26].

$$FC = \frac{\exp\left(-\left(\frac{V_s}{C}\right)^K\right) - \exp\left(-\left(\frac{V_N}{C}\right)^K\right)}{\left(-\left(\frac{V_s}{C}\right)^K\right) - \left(-\left(\frac{V_N}{C}\right)^K\right)} - \left(-\left(\frac{V_A}{C}\right)^K\right) \quad (21)$$

If we obtain a load factor of at least 25%, we can talk about the electrical production of wind turbines.

### 2.9 Wind farm sizing

In order to optimize the operation of wind farms, certain measures must be taken into account. Indeed, the wrong choice of certain parameters can be detrimental to a wind farm. In order to avoid the wake phenomenon, the spacing of wind turbines is taken into account. The installation of wind turbines on a site must take into account the dimensions of the terrain perpendicular and parallel to the predominant wind

direction. The conditions to be respected are as follows from equation (22-24), [4], [9], [27]-[31].

$$10H(N_1 + 1) < IN \quad (22)$$

$$3D(N_2 + 1) < L \quad (23)$$

$$N = N_1 N_2 \quad (24)$$

Where:

$I$ : Dimension of land perpendicular to the predominant wind direction;

$L$ : Dimension of terrain parallel to prevailing wind direction;

$D$ : Machine rotor diameter;

$H$ : Tower height;

$N_1$ : Number of wind turbines per row;

$N_2$ : Number of wind turbines per row;

$N$ : Total number of wind turbines to be placed on site

### 2.10 Application to water pumping

The wind generator produces electrical energy, which powers a pump at the base. Thus, the hydraulic power, which is normally less than or equal to the useful power, is a function of the quantity of water per unit of time required and the total head [30 - 31]. Considering a wind driven pumping system with overall efficiency  $\eta_i$  and total head  $Ht$ , the flow rate of water pumped is given by equation (25).

$$Q = \frac{\eta_i P_{wmax}}{\rho g H_t} \quad (25)$$

The daily flow rate will be equal to equation (26).

$$Q_d = 3600 \times 24 \times \frac{\eta_i P_{wmax}}{\rho g H_t} \quad (26)$$

Another approach to estimating the flow rate without calculating the power supplied by the wind generator is based on the following relationship, equation (27),

$$Q = \int_{V_d}^{V_c} q(v) f(v) dv \quad (27)$$

Where:  $q(v)$ : Curves expressing the variation in pump flow rate to be used as a function of wind speed.

### 2.11 Analysis of wind energy costs

In production technologies, the cost of electricity is primarily affected by three main components.

- Capital and investment cost
- Operating and maintenance cost
- Fuel cost.

Wind energy production benefits from a zero-fuel cost. Studies on the cost of wind energy and other renewable energy sources could become irresponsible due to a lack of understanding of the technology and the economics involved. Misleading comparisons of the costs of different energy technologies are common. The cost of electricity in wind energy production includes the following components [32].

- Economic depreciation of equipment;
- Interest paid on borrowed capital;
- Operating and maintenance cost;
- Taxes paid to local and federal authorities;
- Government incentives and tax credits;
- Royalties paid to landowners;
- Payment for electricity used in standby mode;
- Energy storage components, if applicable.

The Levelized cost of electricity (LCOE) in electric power production can be defined as the present value of the price of the electric energy produced (typically expressed in units of cents per kilowatt-hour), taking into account the economic life of the plant and the costs incurred in construction, operation, and maintenance, as well as fuel costs [32]. The cost of fuel is zero in wind power production, and the wind turbines are assembled in the factory and directly delivered to the wind farm site, resulting in a short construction time,  $t$ . This leads to equation (28), for the LCOE for wind power generation:

$$LCOE = \frac{C_I}{8760 n} \left( \frac{1}{P_R CF} \right) \left[ 1 + m \left\{ \frac{(1+I)^n - 1}{I(1+I)^n} \right\} \right] \quad (28)$$

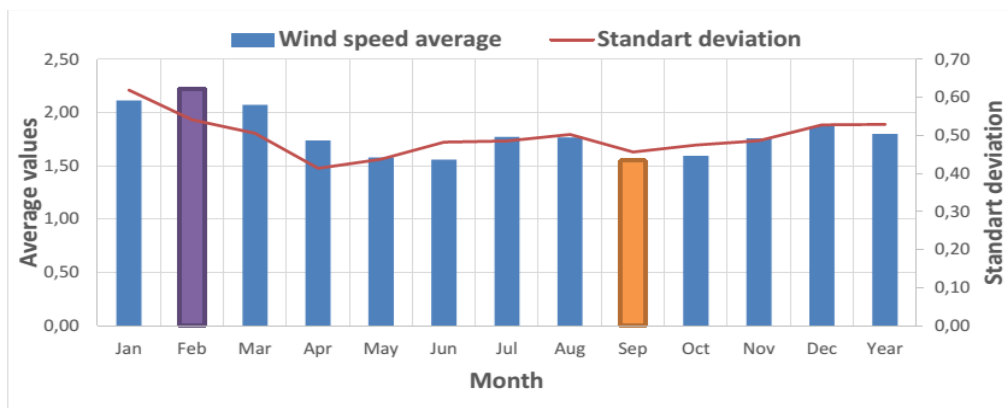


Fig. 2: The wind speed average and standard deviation.

Where,

$I$  = interest rate in %;

$n$  = the lifespan of the turbine;

$m$  = maintenance cost = 15% of the initial investment cost;

The LCOE is estimated over the lifespan of the energy-generating technology, typically 20 years for wind turbines. The discount rate ( $i$ ) is chosen based on the cost and source of available capital, determining a balance between equity and debt financing and an assessment of the financial risks associated with the project (Letcher, 2017) [32]. Table. 1, shows the various costs based on the turbine power.

Table. 1: Initial investment cost based on rated power

Turbine power kW	Cost per kW	Average cost per kW
< 20	2200 - 3000	2600
20 - 200	1250 - 2300	1775
> 200	700 - 1600	1150

### 3 Results and Discussion

#### 3.1. Site wind potential

Wind speed being the essential element for the dimensioning and evaluation of wind turbine power at a site, we modelled the variation in wind speeds, determined the monthly averages of these speeds from 1<sup>st</sup> January 2005 to 31 Dec 2015 and averaged them. Fig. 2, shows a graphical representation of these speeds measured at 10 m above ground level. Wind speed averages vary from 1.55 to 2.22 m/s. The highest wind speeds recorded in the region are in February. The lowest wind speeds are recorded in September.

### 3.2 Weibull parameters

With the wind speeds, the weibull parameters were determined. These are the scale factor  $C$  (m/s) and the shape factor  $K$ . Fig. 3, summarizes the results. The shape factor gives the shape of the distribution and takes a value between 1 and 3. The lower the value, the more variable the wind speed, while a high  $k$  value indicates a constant wind speed. The scale factor expresses the chronology of a characteristic wind

speed. It is proportional to the average wind speed. The shape factor varied between 3.58 and 4.776 this value indicates a constant wind speed

#### 3.2.1 Weibull Distribution

Given the speeds and the parameters  $C$  and  $K$ , we modelled the variation in wind speeds by the probability density function and the distribution function, shown in Fig. 4 and Fig. 5, respectively.

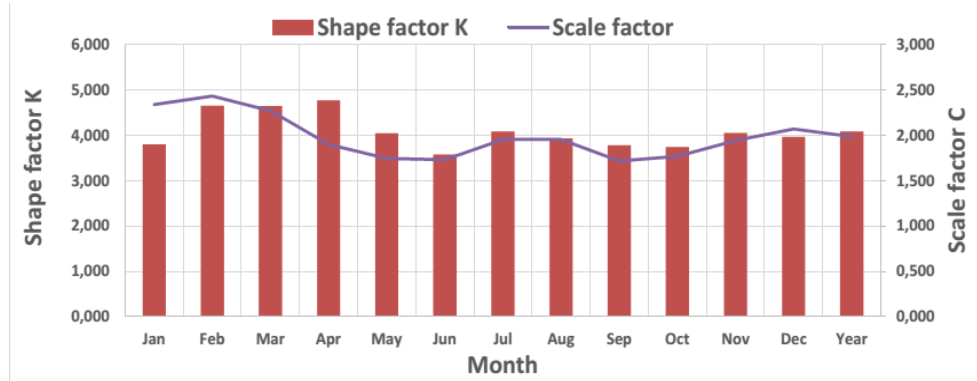


Fig. 3: Shape factor and scale factor.

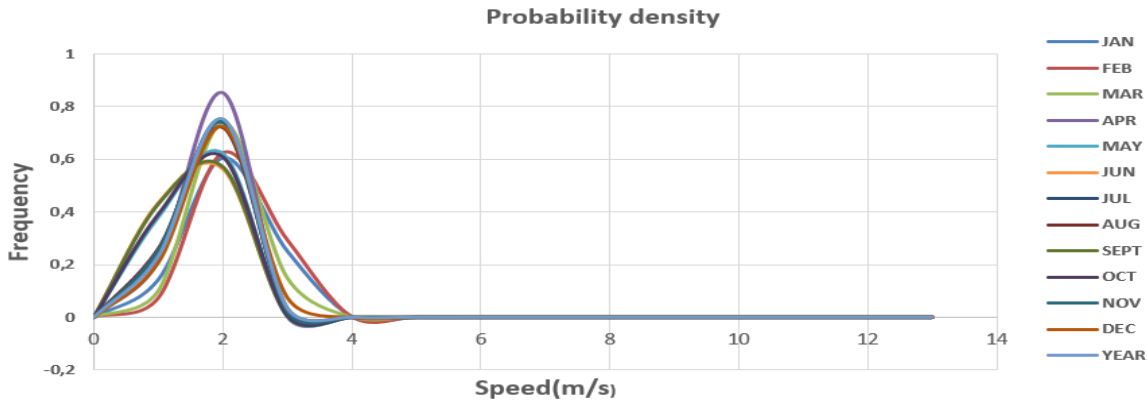


Fig. 4: Probability density curve obtained from wind speeds at 10 m.

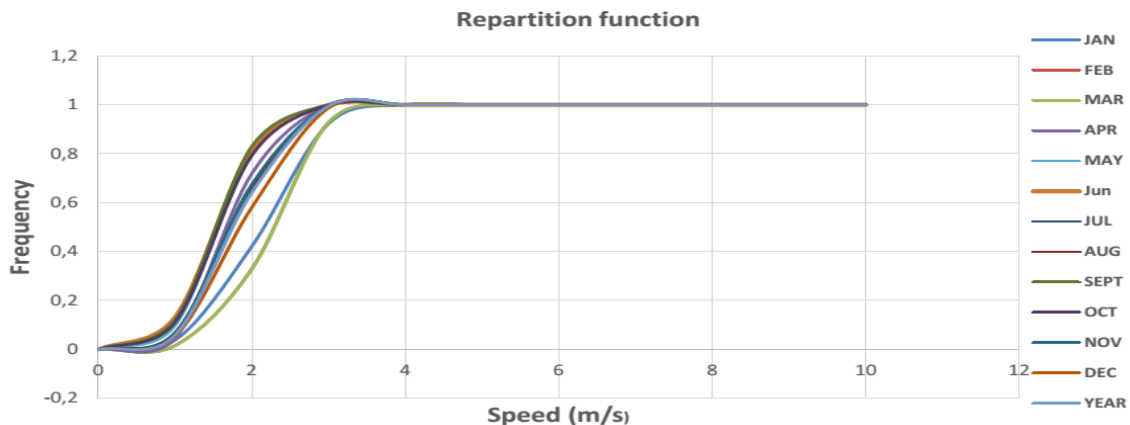


Fig. 5: Distribution function curve obtained from speeds at 10 m above ground level

Fig. 4, shows the probability of a wind blowing at any given speed. The most probable speed is 3 m/s. At a height of 10 m, 68.2% of speeds are below 2.1 m/s, 30.6% of speed data are between 2.1 m/s and 3.6 m/s and only 1.2% are in the range 3.6 m/s to 5 m/s, with the speed range extending slightly up to 5.5 m/s. This figure shows that the average speed is between 2 and 3 m/s, which enables electricity production but with low availability. Wind turbines will find it difficult to reach their rated output, hence the need for extrapolation to obtain favorable speeds. Vertical extrapolation of wind speeds is therefore carried out for heights of 50 m and 100 m, resulting in a variation in wind distribution. If

we look at the shape of the curves, we can see that they are not considerably dispersed. Fig. 5, shows the probability of wind speeds below 4 m/s.

### 3.2.2 Speeds extrapolation

In order to determine the wind speeds that are favorable for energy production in the city of Bertoua, we carried out an extrapolation. Fig. 6, shows the results of the extrapolation of monthly average wind speeds obtained at 10, 20, 30, 40, 50 and 100 m above ground level.

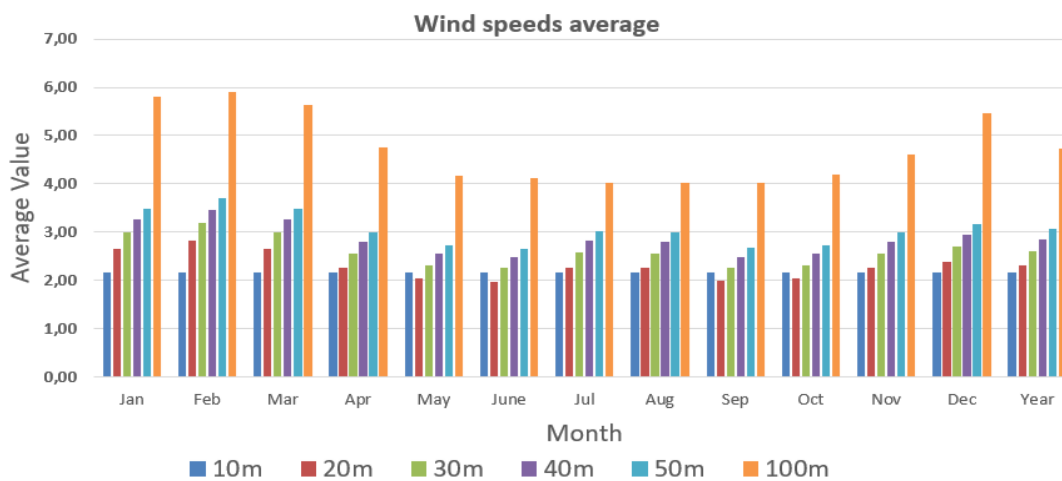


Fig. 6: Extrapolated average monthly wind speed curve.

Table. 2: Extrapolation of Weibull parameters as a function of height

Month	10 m		20 m		30 m		40 m		50 m		100 m	
	c	k	c	k	c	k	c	k	c	k	c	k
JAN	2.34	3.81	2.87	3.83	3.24	3.84	3.53	3.85	3.77	3.86	6.03	5.5
FEB	2.44	4.66	2.98	4.69	3.35	4.7	3.65	4.71	3.89	4.72	6.1	5.74
MAR	2.27	4.65	2.79	4.68	3.15	4.7	3.43	4.71	3.67	4.72	5.86	5.49
APR	1.9	4.78	2.36	4.81	2.68	4.82	2.94	4.83	3.15	4.84	4.93	5.48
MAY	1.75	4.05	2.18	4.08	2.49	4.09	2.73	4.1	2.93	4.11	4.36	4.97
JUN	1.73	3.58	2.17	3.61	2.47	3.62	2.71	3.63	2.91	3.63	4.34	4.73
JUL	1.96	4.09	2.43	4.12	2.75	4.13	3.01	4.14	3.23	4.15	4.19	5.33
AUG	1.96	3.94	2.43	3.96	2.75	3.97	3.01	3.98	3.23	3.99	4.18	5.18
SEP	1.72	3.79	2.15	3.81	2.45	3.82	2.69	3.83	2.89	3.84	4.21	4.81
OCT	1.77	3.74	2.21	3.76	2.52	3.78	2.76	3.79	2.96	3.79	4.37	5.06
NOV	1.94	4.05	2.41	4.08	2.74	4.09	2.99	4.1	3.21	4.11	4.86	4.56
DEC	2.07	3.97	2.56	3.99	2.9	4.01	3.16	4.02	3.39	4.03	5.68	5.35
YEAR	1.99	4.09	2.46	4.12	2.79	4.13	3.05	4.14	3.27	4.15	4.94	5.18

The observation made is that the average speed, which at the beginning, that is to say at 10 m, was insufficient (1.55 to 2.55 m/s), is improving such that as we ascend, the average wind speed increases. At 100 m altitude, the monthly average speed varied between 4.01 and 5.9 m/s. With these speeds, there will be wind energy production in the city of Bertoua. Its average speed values obtained at 100 m classify the city of Bertoua in low zones, which validates the work of (Djiela et al) [4] on wind energy in Cameroon by determining the Weibull parameters: potential of an ecological energy.

### 3.2.3 Extrapolation of Weibull parameters as a function of height

With the parameters  $K$  and  $C$  calculated at 10 meters above ground level, we can extrapolate them based on the height of the site where we want to install the wind turbines. To address this, we use the following formulas in equations (10) and (11), and the values of parameters  $K$  and  $C$  are listed in Table 2. The shape factor varies very little as the height varies positively; unlike the scale factor, which increases considerably as the height increases.

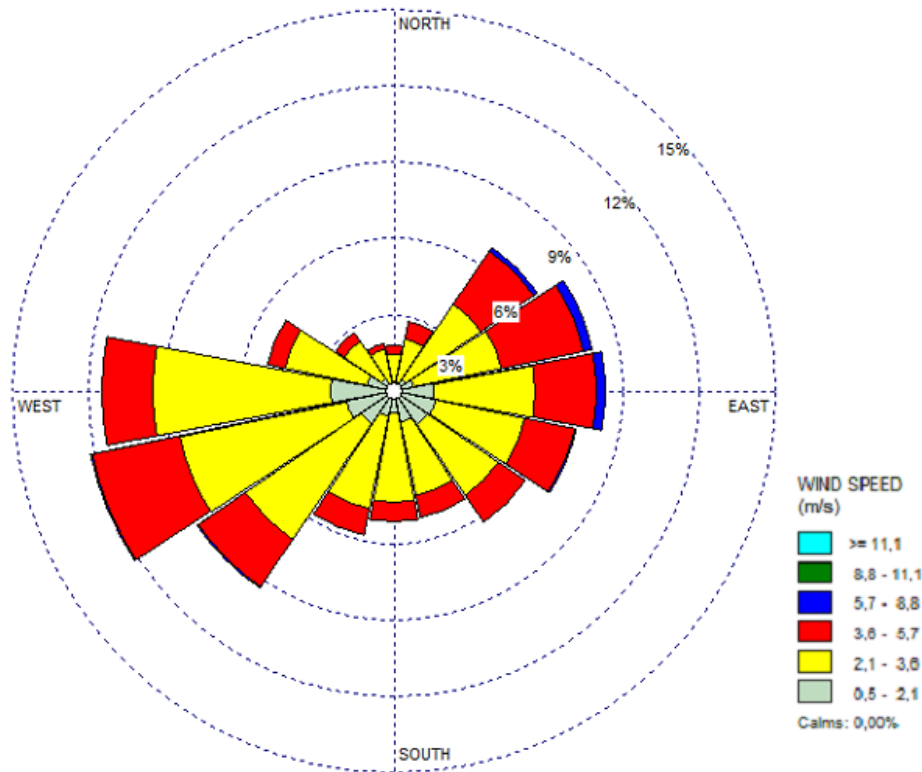


Fig. 7: Monthly and hourly average wind speed.

### 3.2.4 Orientation of wind turbines

The prevailing wind direction in the city of Bertoua is shown in Fig. 7. A look at and analysis of the wind statistics reveals that the wind predominates in the range from West South West (WSW) to East North East (ENE). The highest wind speed, on the other hand, is recorded in the West South West (WSW) direction. Moreover, this interval is the biggest contributor to total energy. Despite a high frequency of speeds in the East South East (ESE) to West North West (WNW) directions, average wind speeds remain low.

Fig. 7 shows the wind rose at the site. Analysis of this curve shows the high probability of wind speeds between 2.1 and 3.6 m/s. As for the annual wind rose at the site, the wind direction is predominantly north-west to south-west. The purpose of these figures is to make better extrapolations in order to obtain wind speeds favorable to the production of electrical energy and the orientation of wind turbines.

## 3.3 Densities, wind power and load factor

### 3.3.1 Energy densities and wind power density

It is used to estimate the recoverable power at a site. Fig. 8 shows the different values depending on the month. For an annual density ranging between 23.44 and 65.45 kW/m<sup>2</sup>/year at 10 m altitude, we had, by making an extrapolation, a density that varies with height: at a height of 100 m, the annual variations go from 325,17 to 1015,97 kW/m<sup>2</sup>/year, with an estimated annual average of 533,97 kWh/m<sup>2</sup>/year. At an altitude of 100 m, the extrapolated wind speeds reached 5.9 m/s, which results in an annual energy density of 1 015.97 kWh/m<sup>2</sup>. This will provide Cameroon with an opportunity to address the energy deficit problem in this region, especially in the months of February and March.

### 3.3.2 Available and recoverable power

#### 3.3.2.1 Available power

In order to determine the wind potential of Bertoua, the variation in wind speed was modelled. Fig 9 and Fig. 10 shows the available and recoverable power at different heights in W/m<sup>2</sup>. An insignificant power at the beginning of 10 m (6.31 W/m<sup>2</sup>), this potential improves with height extrapolation, allowing for a varying available potential with altitude. At a height of 100 m, it ranges from 40.27 to 128.44 W/m<sup>2</sup>, enabling the exploitation of this type of energy in this region, with a maximum in February and a minimum in September.

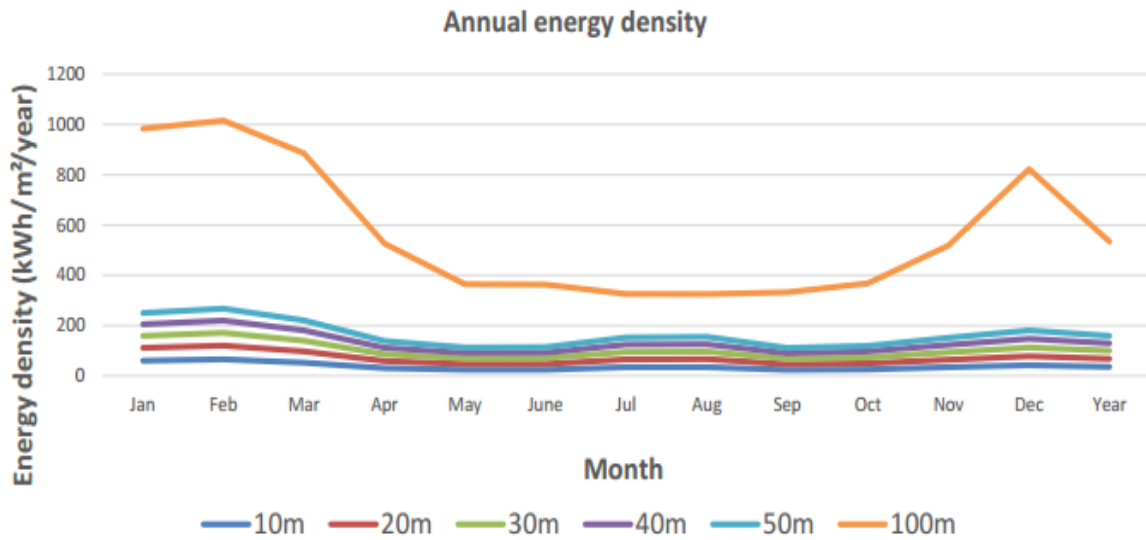


Fig. 8: Annual energy density curves.

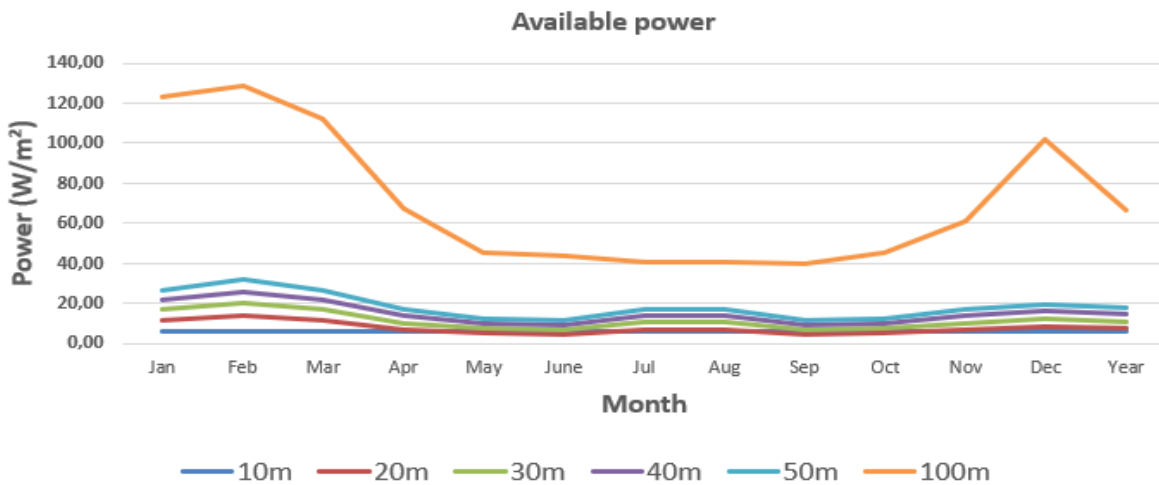


Fig. 9: Available monthly power curves.

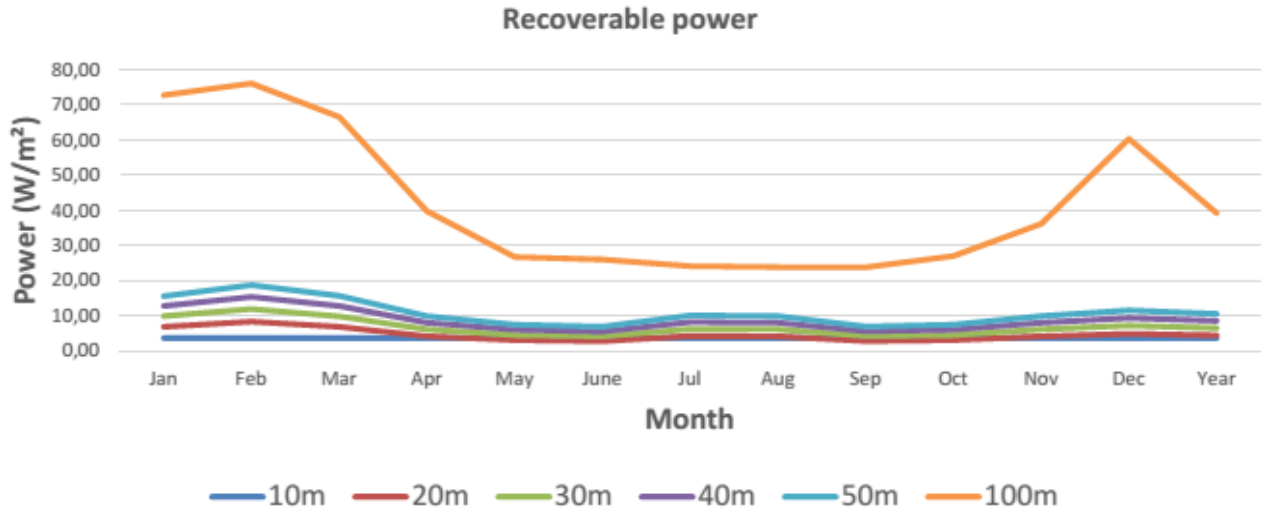


Fig. 10: Monthly recoverable power curves.

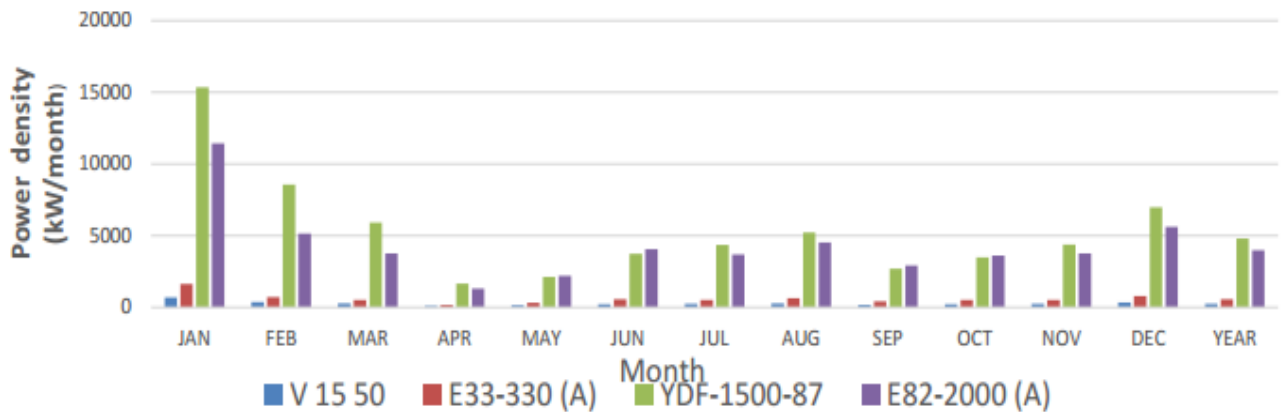


Fig. 11: Variations of the power density at 50 m in the selected site.

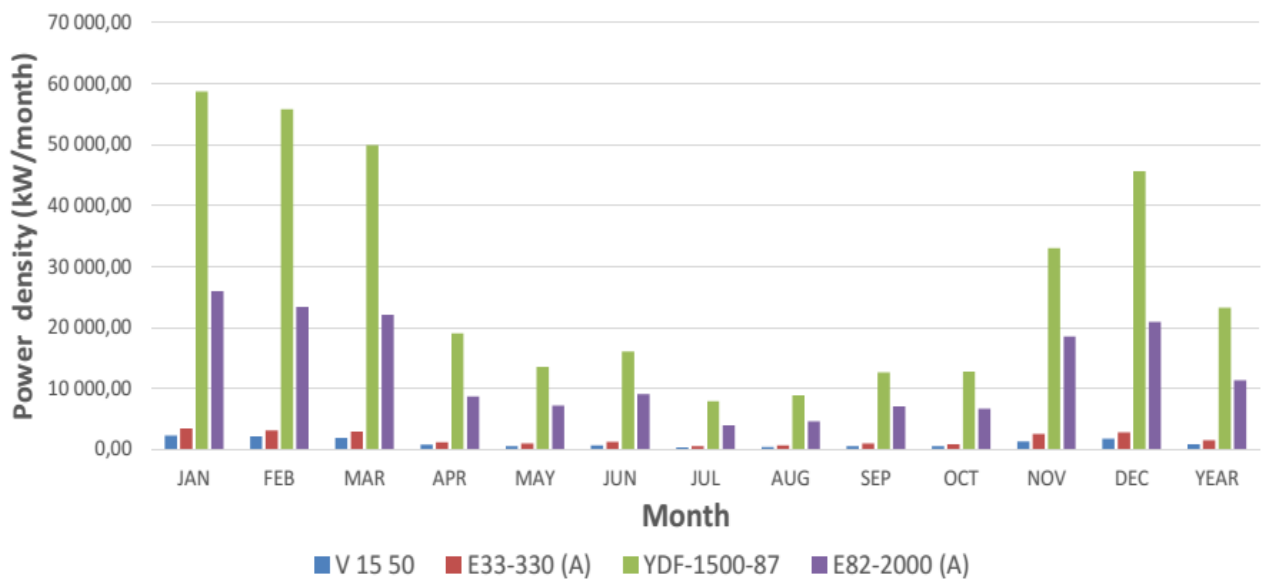


Fig. 12: Variations of the power density at 100 m in the selected site.

### 3.3.2.2 Recoverable power

It is used to estimate the exploitable power at this site after application of the Betz limit. Fig. 12, shows its different values according to the month. The recoverable potential at a height of 100 m varies between 23.87 and 76.11W/m<sup>2</sup>, with maximums in February and minimums in September.

### 3.3.3 Suitable wind generator and load factor

#### 3.3.3.1 Choosing the most suitable wind generator technology

As the blades are located at hub level, the height of the wind turbine mast must be taken into account for power calculations. Four types of wind turbines were selected to determine which would produce the most power. Table. 3 shows the characteristics of the wind turbines. These include turbine type, manufacturing company, country of manufacture, power, rotor diameter, mast height and operating speeds.

**Table. 3:** Types of wind turbines selected for the park model.

Features	V 1550	Enercon	YDF-1500-87	Enercon
	Vergnet (F)	E33-330 (A)	CNYD (C)	E82-2000 (A)
Height (m)	60 m	50 m	75 m	130 m
Power (kW)	50	330	1500	2000
Diameter (m)	15.2	33.4	87	82
V <sub>s</sub> (m/s)	2.5	2.5	3	2.5
V <sub>N</sub> (m/s)	10	13	10.2	12.5
V <sub>A</sub> (m/s)	25	25	25	25

To match the park model with a real wind turbine, we have selected four (04) types of wind turbine, 02 of medium power and 02 of high power. Fig. 11 and Fig. 12 show the evolution of power density at heights of 50 m and 100 m, respectively, as a function of month, for each of the wind turbines. The curves show the same pattern, the only difference being that the higher the wind turbine, the higher the density. The months from November to March show the highest power density values. And the YDF-1500-87 wind generator will produce more energy than the others at its various heights. The turbine YDF-1500-87 wind generator remains the best compromise because it produces more energy than the others as Kidmo et al. [3] applied the same method in the northern region of Cameroon and achieved the best production with this turbine.

#### 3.3.3.2 Load factor

Fig. 13, shows the load factor curve as a function of height and turbine type. Its value increases with the height of the wind turbine installation site. It varies between 0.06 and 2.5, values that are acceptable for energy production. Fig. 14, shows the variation in usable power produced by the YDF-500-87 wind turbine installed at different heights. Of the four (04) types we had chosen to simulate their production, this one is the best because it has a good load factor and produces more energy than the other three. This wind turbine guarantees production in January of 82.66 kW at 100 m altitude.

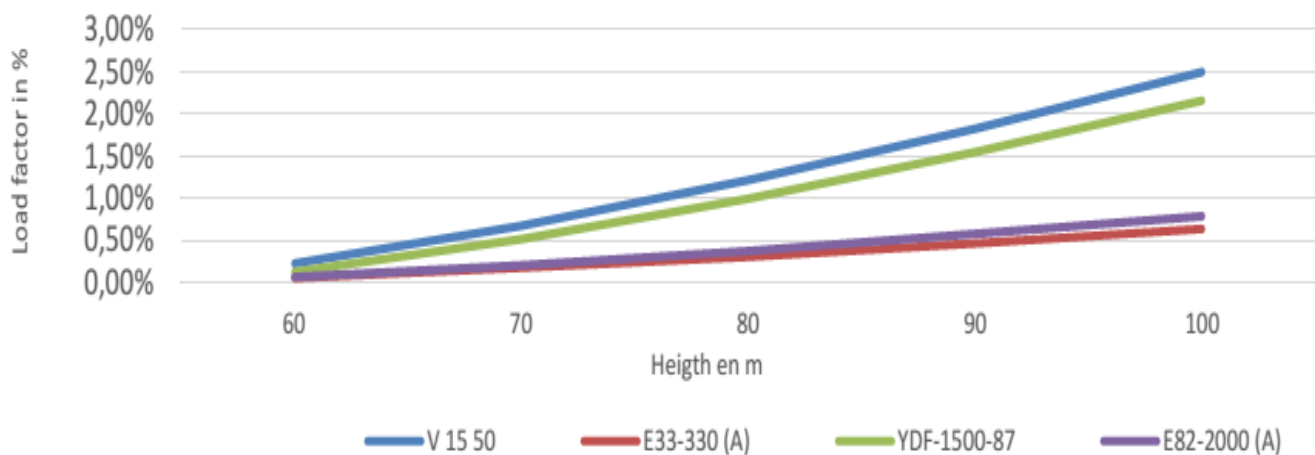


**Fig. 13:** Variations of the load factor as a function of height and turbine type.

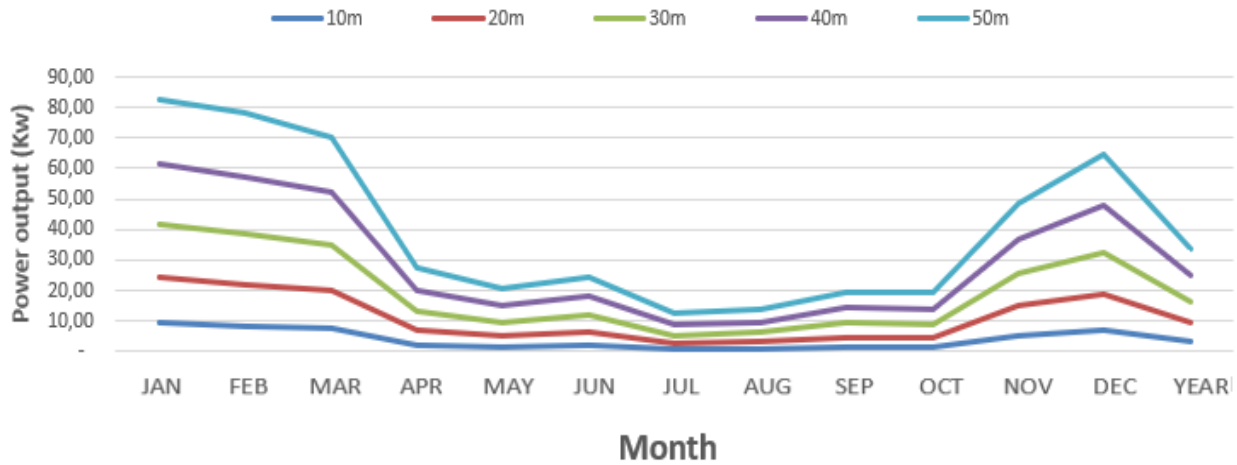


Fig. 14: YDF-1500-87 wind turbine power output trend.

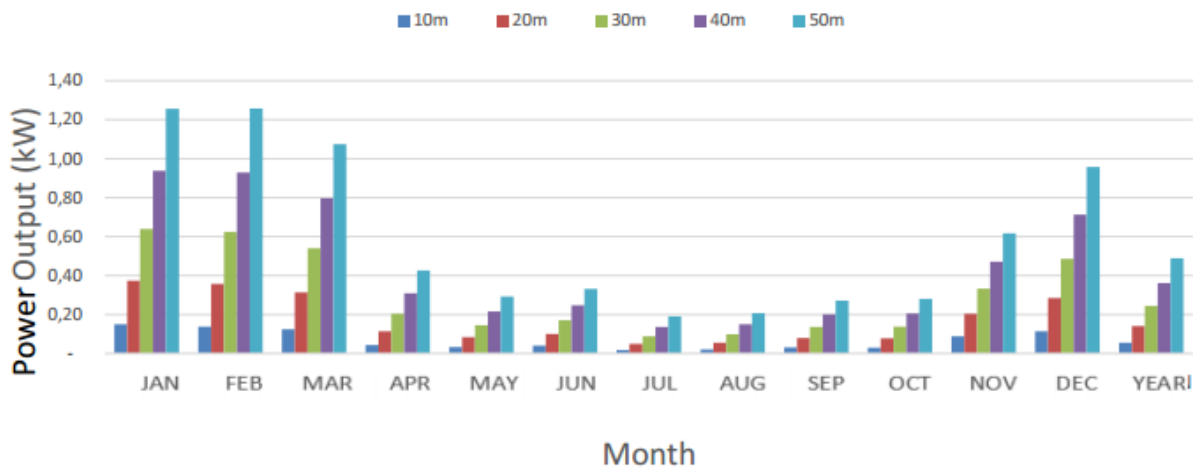


Fig. 15: CF 6e wind turbine power output trend.

Water flow produced is shown in Fig. 16. It will produce more from November to March, when there is greater energy demand in Cameroon in general, due to lower water levels in the hydroelectric dams. This study is part of the strategies to research solutions in order to replace fossil fuels used for energy production in the East region in general and the city of Bertoua in particular. It is beneficial because it produces more between November and March, which will be an asset for this region, as it is during this period that there is a drop in water levels throughout Cameroon in general, leading to a decrease in energy production across the country, hence, searching for other production possibilities is a necessity.

### 3.4 Application to water pumping

For this section, we obtained the following: The useful power produced by a CF 6e wind turbine

intended for water pumping is represented in the following Fig. 15. Usable power at a height of 50 m varies between 0.2 and 1.3kW. In other words, the turbine will operate at a maximum of 21.66% of its rated speed. The greater the total dynamic head, the less significant the volume of water that can be extracted per day.

### 3.5 Analysis of wind energy costs

For a turbine with an initial investment of 3,900,000 (USD cents), an interest rate of 12%, a lifespan of 20 years, and a maintenance rate of 20%, we obtain the various energy costs. The cost of energy varies between 443.74 XAF in January and 3018.54 XAF in July, with an annual average of 1081.56 XAF, which is acceptable considering the values of Trevor M. Letcher [32] (Table. 1), who sets the average cost of energy based on the installed power at a site, shown in Fig. 17.

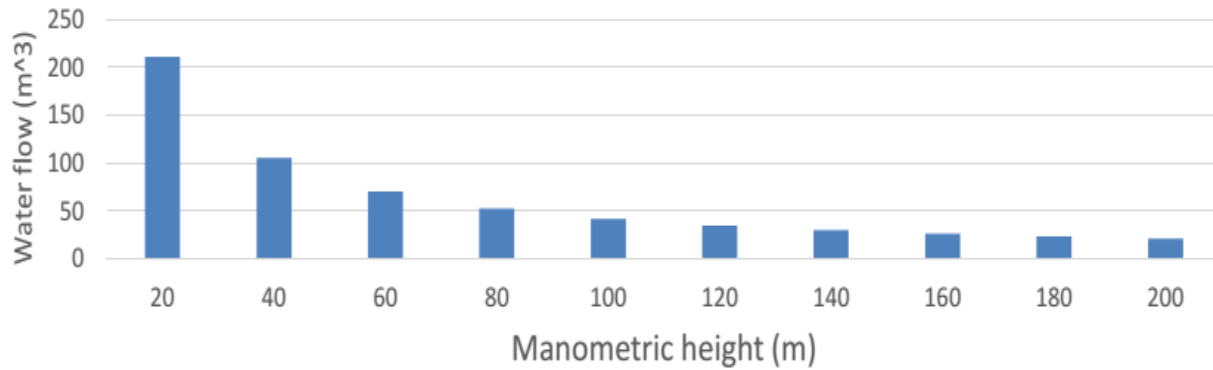


Fig. 16: Water flow produced from the CF 6th wind turbine at an altitude of 50 meters.

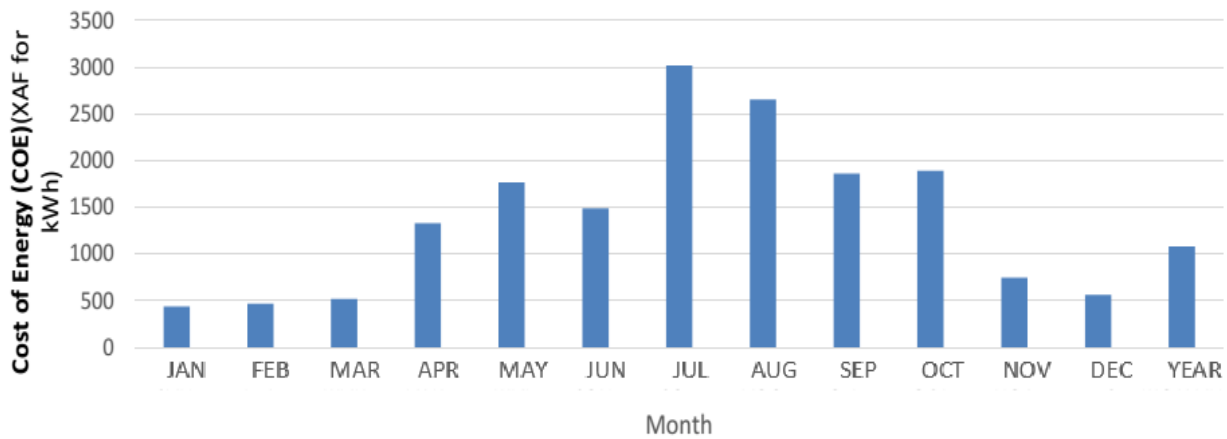


Fig. 17: The cost of energy.

The results obtained in this article show that the city of Bertoua, despite being classified as a low wind speed area, has the potential for energy production at an altitude of 100 m, which could replace the current energy production that primarily relies on thermal power plants and hydroelectric dams. It will also be a question of modeling a wind turbine conversion chain and establishing a complete control strategy using artificial intelligence to optimize the system's performance with a view to ensuring its injection into the existing power grid, since this alone will not be enough to meet the energy demand of the East Cameroon region.

#### 4 Conclusion

The work carried out in this article provided an overview of the feasibility and study of the integration of wind energy in the locality of Bertoua. A turbine model was used to validate the results in order to understand the types of equipment and methods to use. Certain parameters were taken into account, such as

altitude and wind speed. Our analysis shows that the wind at the site is consistent and propagates in a North North East (NNE) direction, with stable average speeds ranging from 1.55 m/s to 2.22 m/s at an altitude of 10 m for a very low usable power of 3.74 W/m<sup>2</sup>. The best average wind speeds of 4.03 to 5.9 m/s, favorable for good electricity production, are obtained by extrapolation at altitudes of 100 m corresponding to the heights of the masts. We obtain an annual energy density ranging from 325.17 to 1015.97 kWh/m<sup>2</sup>, based on the potential deposition of the studied site. Furthermore, the wind energy of the city in question predicts that the YDF-1500-87 CNYD generator is the right machine to install, as it has a better capacity factor than others, ensuring useful electric energy production of up to 82.66 kW per machine installed in this city. Although the locality of Bertoua does not facilitate high-capacity wind energy production, this study has not only reassured the financiers but has also demonstrated the possibility of using small power plants for dedicated use in water pumping and for

small energy consumers. Maximum production during the period when energy demand in Cameroon is very high will help reduce production from thermal power plants, thereby reducing the CO<sub>2</sub> and sulfur emissions that these plants release. It will be a matter of looking into the possibility of integrating this study into the other departments of the Eastern region of Cameroon in order to map the wind potential of this region and to develop this form of energy in Cameroon.

### Acknowledgment

We thank the international airport of Bertoua for providing us with the meteorological data that enabled us to carry out this study.

### Data Availability Statement

The data supporting the results of this study are available on request from the author, Doka Baza Gilbert, the corresponding author.

### Conflict of Interest

Authors state “No conflict of interest”.

### CRedit authorship contribution statement

Conceptualization, DBG, JBB, ADP, SH, BTPR, K, DKK, and NJL; methodology, DBG.; software, ADP; validation, SH, BTPR and K; formal analysis, DKK; investigation, NJL; resources, JBB; data curation, SH; writing—original draft preparation, DBG; writing—review and editing, K; visualization, BTPR; supervision, NJL; project administration, DBG; funding acquisition, K. All authors have read and agreed to the published version of the manuscript.

### References

[1] T. Louossi, Kitmo, F. F. G. Armel, N. Arnaud, D. B. Gilbert, H. M. Soulouknga, and F. T. Ahmed, “Study method of the P&O algorithm using pulse width modulation and duty cycle modulation: application to the search for the maximum power point of PV systems”, *International Transactions on*

*Electrical Engineering and Computer Science*, Vol. 4, No. 4, pp. 175–182, December 2025.

<https://doi.org/10.62760/iteecs.4.4.2025.156>

[2] Kitmo, A. D. Pene, B. Jacques, J. B. Bidias, T. Louossi, D. B. Gilbert, K. K. Dieudonne, J. L. Nsouandele, N. Djongyang, and C. Kapseu, “A robust maximum power point tracking control under shading effects on photovoltaic systems”, *International Transactions on Electrical Engineering and Computer Science*, Vol. 4, No. 3, pp. 137–151, September 2025.

<https://doi.org/10.62760/iteecs.4.3.2025.144>

[3] D. K. Kidmo, K. Deli, D. Raidandi, and S. D. Yamigno, “Wind energy for electricity generation in the far north region of Cameroon”, *Energy Procedia*, Vol. 93, pp. 66–73, August 2016.

<https://doi.org/10.1016/j.egypro.2016.07.151>

[4] R. H. T. Djiela, P. T. Kapen, and G. Tchuen, “Wind energy of Cameroon by determining Weibull parameters: potential of a environmentally friendly energy”, *International Journal of Environmental Science and Technology*, Vol. 18, pp. 2251–2270, 2021.

<https://doi.org/10.1007/s13762-020-02962-z>

[5] O. A. Marzouk, “Wind speed weibull model identification in Oman, and computed normalized annual energy production from wind turbines based on data from weather stations”, *Engineering Reports*, Vol. 7, No. 3, art. no. e70089, March 2025.

<https://doi.org/10.1002/eng2.70089>

[6] A. K. Yadav, V. Yadav, U. Kumar, A. Ranjan, T. S. V. Kumar, R. Khargotra, G. Fekete, and T. Singh, “Analysis of wind power generation potential and wind turbine installation economics: A correlation-based approach”, *Results in Engineering*, Vol. 25, art. no. 103743, 2025.

<https://doi.org/10.1016/j.rineng.2024.103743>

[7] B. S. Ndeba, O. E. Alani, A. Ghennioui, and M. Benzaazoua, “Comparative analysis of seasonal wind power using Weibull, Rayleigh and Champernowne distributions”, *Scientific Reports*, Vol. 15, art. no. 2533, January 2025.

<https://doi.org/10.1038/s41598-025-86321-3>

[8] I. Hussain, A. Haider, Z. Ullah, M. Russo, G. M. Casolino, and B. Azeem, “Comparative analysis of eight numerical methods using weibull distribution to estimate wind power density for

- coastal areas in Pakistan”, *Energies*, Vol. 16, No. 3, art. no. 1515, February 2023.  
<https://doi.org/10.3390/en16031515>
- [9] J. Wan, F. Zheng, H. Luan, Y. Tian, L. Li, Z. Ma, Z. Xu, and Y. Li, “Assessment of wind energy resources in the urat area using optimized weibull distribution”, *Sustainable Energy Technologies and Assessments*, Vol. 47, art. no. 101351, 2021.  
<https://doi.org/10.1016/j.seta.2021.101351>
- [10] S. Deep, A. Sarkar, M. Ghawat, and M. K. Rajak, “Estimation of the wind energy potential for coastal locations in India using the Weibull model”, *Renewable Energy*, Vol. 161, pp. 319-339, December 2020.  
<https://doi.org/10.1016/j.renene.2020.07.054>
- [11] H. Teimourian, M. Abubakar, M. Yildiz, and A. Teimourian, “A comparative study on wind energy assessment distribution models: a case study on Weibull distribution”, *Energies*, Vol. 15, No. 15, art. no. 5684, august 2022.  
<https://doi.org/10.3390/en15155684>
- [12] M. A. Alanazi, M. Aloraini, M. Islam, S. Alyahya, and S. Khan, “Wind energy assessment using weibull distribution with different numerical estimation methods: a case study”, *Emerging Science Journal*, Vol. 7, No. 6, pp. 2260–2278, December 2023.  
<https://doi.org/10.28991/ESJ-2023-07-06-024>
- [13] P. Crippa, M. Alifa, D. Bolster, M. G. Genton, and S. Castruccio, “A temporal model for vertical extrapolation of wind speed and wind energy assessment”, *Applied Energy*, Vol. 301, art. no. 117378, November 2021.  
<https://doi.org/10.1016/j.apenergy.2021.117378>
- [14] O. J. Mdee, “Performance evaluation of Weibull analytical methods using several empirical methods for predicting wind speed distribution”, *Energy Sources, Part A: Recovery, Utilization, and Environmental Effects*, Vol. 47, No. 1, pp. 1626–1649, June 2025.  
<https://doi.org/10.1080/15567036.2020.1832161>
- [15] W. Wang, Y. Gao, and N. Ikegaya, “Approximating wind speed probability distributions around a building by mixture weibull distribution with the methods of moments and L-moments”, *Journal of Wind Engineering and Industrial Aerodynamics*, Vol. 257, art. no. 106001, February 2025.  
<https://doi.org/10.1016/j.jweia.2024.106001>
- [16] A. R. Shoib, D. H. Didane, A. N. Mohammed, K. Abdullah, and M. F. M. Ali, “Technical assessment of wind energy potentiality in Malaysia using Weibull distribution function”, *Journal of Advanced Research in Fluid Mechanics and Thermal Sciences*, Vol. 86, No. 1, pp. 1–13, October 2021.  
<https://doi.org/10.37934/arfmts.86.1.113>
- [17] M. Albassam, M. Ahsan-Ul-haq, and M. Aslam, “Weibull distribution under indeterminacy with applications”, *AIMS Mathematics*, Vol. 8, No. 5, pp. 10745–10757, 2023.  
<https://doi.org/10.3934/math.2023545>
- [18] Z. Sedliačková, I. Pobočíková, M. Michalková, and D. Jurášová, “Wind speed modeling using Weibull distribution: A case of Liptovský Mikuláš, Slovakia”, *MATEC Web of Conferences*, Vol. 357, art. no. 08005, June 2022.  
<http://doi.org/10.1051/mateconf/202235708005>
- [19] S. M. A. Aljeddani and M. A. Mohammed, “A novel approach to Weibull distribution for the assessment of wind energy speed”, *Alexandria Engineering Journal*, Vol. 78, pp. 56–64, September 2023.  
<https://doi.org/10.1016/j.aej.2023.07.027>
- [20] H. Z. Muhammed and E. M. Almetwally, “Bayesian and Non-Bayesian estimation for the bivariate inverse Weibull distribution under progressive Type-II censoring”, *Annals of Data Science*, Vol. 10, pp. 481-512, 2023.  
<https://doi.org/10.1007/s40745-020-00316-7>
- [21] Y. W. Koholé, R. H. T. Djiela, F. C. V. Fohagui, and T. Ghislain, “Comparative study of thirteen numerical methods for evaluating Weibull parameters for solar energy generation at ten selected locations in Cameroon”, *Cleaner Energy Systems*, Vol. 4, art. no. 100047, April 2023.  
<https://doi.org/10.1016/j.cles.2022.100047>
- [22] P. E. Agbonifo, “Renewable energy development: Opportunities and barriers within the context of global energy politics”, *International Journal of Energy Economics and Policy*, Vol. 11, No. 2, pp. 141–148, 2021.  
<http://doi.org/10.32479/ijeep.10773>
- [23] I. Akhtar, S. Kirmani, and M. Jameel, “Reliability assessment of power system considering the impact of renewable energy sources integration

- into grid with advanced intelligent strategies”, *IEEE Access*, Vol. 9, pp. 32485–32497, 2021.  
<http://doi.org/10.1109/ACCESS.2021.3060892>
- [24] Y. E. Khchine, M. Sriti, and N. E. E. K. Elyamani, “Evaluation of wind energy potential and trends in Morocco”, *Heliyon*, Vol. 5, No. 6, art. no. e01830, June 2019.  
<https://doi.org/10.1016/j.heliyon.2019.e01830>
- [25] N. A. P. Londo, D. S. L. Londo, R. O. Hugo, F. Londo, N. S. Salcán, D. K. Campoverde-Santos, D. Quingatuña, J. Coello-Cabezas “Estimation of Weibull distribution parameters to assess the wind energy potential of high altitude sites in the Andean region of Ecuador”, *Results in Engineering*, Vol. 27, art. no. 106053, September 2025.  
<https://doi.org/10.1016/j.rineng.2025.106053>
- [26] H. Benbouhenni and N. Bizon, “A synergetic sliding mode controller applied to direct field-oriented control of induction generator-based variable speed dual rotor wind turbines”, *Energies*, Vol. 14, No. 15, art. no. 4437, August 2021.  
<https://doi.org/10.3390/en14154437>
- [27] S. M. S. Alavi, A. Maleki, A. Noroozian and A. Khaleghi, “Simultaneous optimal site selection and sizing of a grid-independent hybrid wind/hydrogen system using a hybrid optimization method based on ELECTRE: A case study in Iran”, *International Journal of Hydrogen Energy*, Vol. 55, pp. 970-983, February 2024.  
<https://doi.org/10.1016/j.ijhydene.2023.11.110>
- [28] A. M. Gómez, K. Morozovska, T. Laneryd, and P. Hilber, “Optimal sizing of the wind farm and wind farm transformer using MILP and dynamic transformer rating”, *International Journal of Electrical Power and Energy Systems*, Vol. 136, art. no. 107645, 2022.  
<https://doi.org/10.1016/j.ijepes.2021.107645>
- [29] Y. F. Nassar, M. J. Abdunnabi, M. N. Sbeta, A. H Ahmad, K. A. Amer, A. Y. Ahmed, and B. Belgasim, “Dynamic analysis and sizing optimization of a pumped hydroelectric storage-integrated hybrid PV/Wind system: A case study”, *Energy conversion and management*, Vol. 229, art. no. 113744, 2021.  
<https://doi.org/10.1016/j.enconman.2020.113744>
- [30] F. Greco, S. G. J. Heijman, and A. Jarquin-Laguna, “Integration of wind energy and desalination systems: A review study”, *Energies*, Vol. 9, No. 12, art. no. 2181, 2021.  
<https://doi.org/10.3390/pr9122181>
- [31] N. Melián-Martel, B. D. Río-Gamero, and J. Schallenberg-Rodríguez, “Water cycle driven only by wind energy surplus: Towards 100% renewable energy islands”, *Desalination*, Vol. 515, art. no. 115216, 2021.  
<https://doi.org/10.1016/j.desal.2021.115216>
- [32] T. M. Letcher, “Why Wind Energy?”, *Wind Energy Engineering*, pp. 3–14, 2017.  
<https://doi.org/10.1016/B978-0-12-809451-8.00001-1>



**Copyright:** © 2026 by the authors, Licensee ITEECS, India. This article is an open access article distributed under the terms and conditions of the Creative Commons Attribution (CC BY) license (<https://creativecommons.org/licenses/by/4.0/>).

\*\*\*